Moment loading of caissons installed in saturated sand

Felipe A. Villalobos, Byron W. Byrne & Guy T. Houlsby
Department of Engineering Science, Oxford University

ABSTRACT: A series of moment capacity tests have been carried out at model scale, to investigate the effects of different installation procedures on the response of suction caisson foundations in sand. Two caissons of different diameters and wall thicknesses, but similar skirt length to diameter ratio, have been tested in water-saturated dense sand. The caissons were installed either by pushing or by using suction. It was found that the moment resistance depends on the method of installation.

1. INTRODUCTION

Suction caisson foundations are increasingly being used in offshore applications. They have been used for fixed structure applications, as described by Bye *et al.* (1995), and also for floating facilities (House, 2002). More recently they are being considered as foundations for offshore wind turbines (Byrne and Houlsby, 2003). The wind turbine structures may be founded on single or multiple caissons. The multiple caisson problem is addressed by Kelly *et al.* (2004), so in this paper we concentrate on the single caisson problem. Typical dimensions and loads for this problem are shown in Figure 1. Byrne and Houlsby (2003) describe this problem in detail, but the main differences in loads on the foundations for offshore wind turbines as compared to typical oil and gas structures are that: (a) the vertical load is much smaller, (b) the horizontal and moment loads are proportionately larger. New design methods must be developed to allow safe designs to be engineered for this regime of loading. As a result Byrne *et al.* (2002) describe a research project aimed at developing such design guidelines. This paper outlines the results from a part of that project.

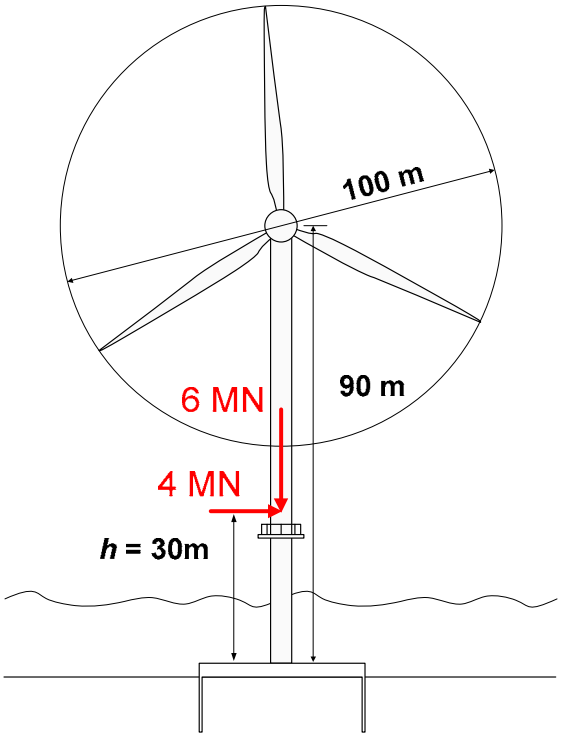

Figure 1: Dimensions and magnitude of loads for a 3.5MW turbine structure founded on a monopod suction (adapted from Byrne and Houlsby, 2003)

Initial studies of the moment capacity of caisson foundations in the laboratory were carried out in drained sand. Preliminary results from these experiments are described by Byrne *et al.* (2003). As the sand used during the tests was dry, the caissons were installed into the prepared sand bed by applying a vertical load. The advantage of using dry sand is that the test bed can be prepared quickly, and a large number of tests can be carried out at specified densities. To mitigate the effects of scale, the tests beds were chosen to be relatively loose. Clearly using installation by applying vertical loads is different from the procedure that has to be used in the field *i.e.* the suction installation process. The different installation techniques may impose different stress paths on elements of soil around the caisson, which in turn may affect the response of the caisson to the applied loads. Therefore it is necessary to carry out experiments similar to those

in the dry sand, but on caissons installed by suction, to observe if there are any fundamental differences in behaviour.

Combined vertical, moment and horizontal loading tests have been conducted on caissons installed by suction and by vertical load in a water-saturated, dense sand. Load-displacement data are presented and interpreted for installation and for moment loading tests.

2. EQUIPMENT AND MATERIALS

2.1 Sand samples

The sand used during the experiments was a commercially produced sand called Redhill 110. The properties of this sand are given in Table 1.

Table 1: Redhill 110 properties (Kelly *et al.*, 2004)

D_{10}, D_{30}, D_{50}, D_{60} (mm)	0.08, 0.10, 0.12, 0.13
Coefficients of uniformity, C_u and curvature C_c	1.63, 0.96
Specific gravity, G_s	2.65
Minimum dry density, γ_{min} (kN/m^3)	12.76
Maximum dry density, γ_{max} (kN/m^3)	16.80
Critical state friction angle, ϕ_{cs}	36º

The sand samples were saturated with water inside a tank of diameter 1100mm and depth 400mm. Preparation of the test bed involved an initial phase of fluidisation by an upward hydraulic gradient induced in the sand bed. The sample was then densified by vibration under a small confining stress. The density was determined by measuring the weight and the volume of the sample. The preparation process was halted once a target density was reached. The peak triaxial angle of friction was estimated as 44.1º to 45.2º from the correlation of Bolton (1986), for the range of relative densities tested (see Table 3).

2.2 Testing procedure

Tests were performed using a three degree-of-freedom loading rig (3DOF) designed by Martin (1994). This rig, shown in Figure 2, can apply any combination of vertical, rotational and horizontal displacement (w, $2R\theta$, u) to a footing by means of computer-controlled stepper motors (R is the radius of the footing). Byrne (2000) has installed a software control program, so that any combination of vertical, moment or horizontal load (V, $M/2R$, H) can also be applied to the footing. All displacements and loads are monitored and recorded using appropriate data-acquisition routines as well as being used within feedback control routines. It is possible to apply

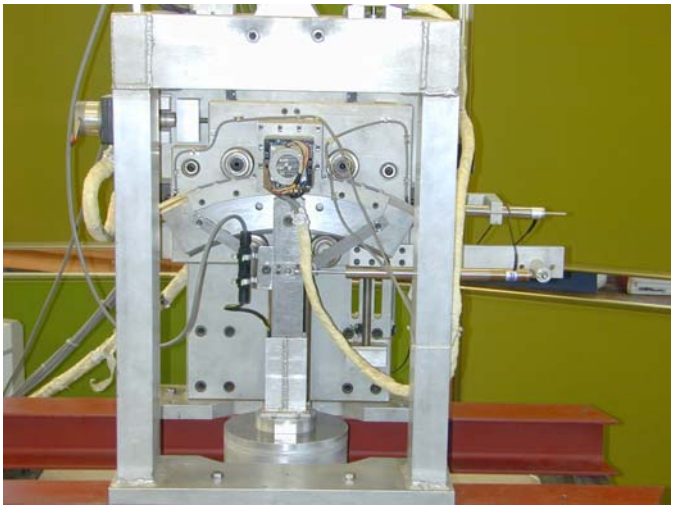

Figure 2: 3DOF-loading rig

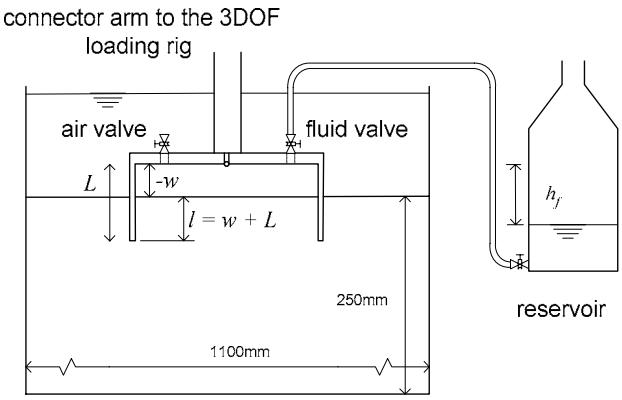

Figure 3: Suction device

loads and displacements to the footing which represent the offshore environment loads of gravity, wind, waves and currents. The geometry of the model suction caissons used in the experiments is given in Table 2. The model caissons were fabricated from aluminium alloy, with a relatively smooth (but not polished) surface.

Table 2: Geometry of the model caissons tested

Diameter, $2R$ (mm)	293	200
Length of skirt, L (mm)	146.5	100
Thickness of the skirt wall, t (mm)	3.4	1.0
Aspect ratio, $L/2R$	0.5	0.5
Thickness ratio, $2R/t$	86	200

The loading apparatus was modified to allow the footings to be suction installed. Previous experiments had only used caissons forced into the ground by vertical load. To enable the suction installation phase to be carried out, the equipment was modified as shown in Figure 3. The suction caisson, attached to the 3DOF loading rig, was pushed into the ground about 30mm with the air valve open. This allowed the pressure inside the

caisson to equilibrate to the outside pressure. On reaching a penetration of 30mm the air valve was closed, and the fluid valve opened. The fluid from inside of the caisson was connected to a reservoir, which was slowly lowered to increase the head difference, h_f, between the inside and outside of the caisson. The head difference was increased to a maximum of 300mm (3kPa), whilst the vertical load applied to the footing was kept constant using feedback control. The reservoir was connected to the suction caisson by a pipe of 6mm internal diameter, chosen to allow sufficient water flow with minimal head loss.

This procedure allowed the caisson to be installed by suction whilst connected to the loading rig. Once the suction phase was complete, it was possible to carry out experiments similar to those carried out on the dry sand as described by Byrne *et al.* (2003).

2.3 Comments on Installation Methods

The two different installation methods have been described by Houlsby and Byrne (2005). Installation by vertical load involves pushing the caisson into the ground. The resistance to penetration is given by the friction on the inside and outside of the wall, and the bearing resistance on the skirt tip. Due to 'silo effects' the stresses around the skirt, and at the tip, are enhanced, leading to larger resistances than may be given by a more conventional pile calculation. Houlsby and Byrne (2005) developed expressions for predicting the resistance to penetration for caissons, taking account of these 'silo' effects. The equations they developed are used below to provide a comparison with the experimental results. In these calculations it will be assumed that $(K\tan\delta)_{i,o}$ takes a value of 0.9, and the stress enhancement factors m and n are taken as 1.

Installation by suction requires an initial penetration to create a seal at the skirt tip. Typically 10% to 20% of the caisson skirt penetrates into the ground under its own weight. The seal allows the suction process to begin and should prevent the occurrence of an unconfined flow failure (*i.e.* a piping failure). Once sealed, the caisson will penetrate into the ground under the application of suction. Typically a pump will remove fluid from inside the caisson, creating a pressure differential on the caisson lid, as well as inducing hydraulic gradients in the soil. The hydraulic gradients lead to changes in the effective stresses around the caisson skirt that are beneficial to installation. Houlsby and Byrne (2005) have developed expressions to calculate the required suction for installation of caissons. This expression is used below for comparison with the experimental data.

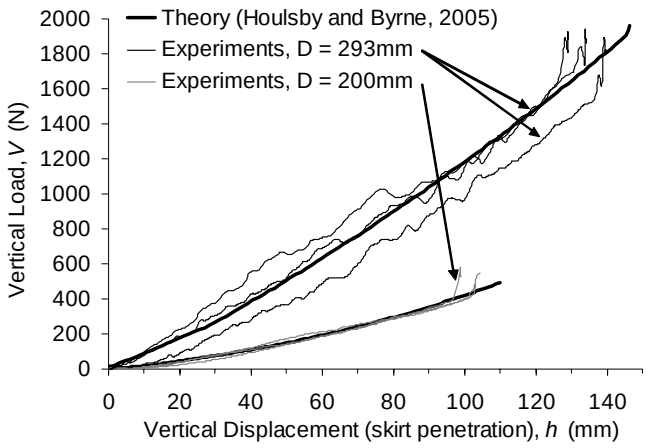

Figure 4: Pushing installation tests and theoretical calculations for both caissons

4. RESULTS OF THE INSTALLATION TESTS

Figure 4 shows the load-displacement results for caissons pushed into the ground at a constant rate. The results are shown as vertical load V against vertical penetration h. The maximum values of V obtained during these tests were approximately 400N for the footing of diameter 200 mm and 1700N for the 293 mm diameter footing. These maximum values of V (denoted by V_o in Table 3) represent "preconsolidation" vertical loads which might be used for interpreting the results within the context of a yield surface model (Gottardi *et al.*, 1999; Houlsby and Cassidy, 2002). R_d in Table 3 is the Relative Density. Also shown on Figure 4 is a theoretical prediction calculated using the methods of Houlsby and Byrne (2005).

Table 3: Installation tests (**S**uction and **P**ushing)

Test	$2R$ mm	V N	V_o N	R_d %	$\dot{h}$ mm/s
FV6_5_1S	200	5	398	75	0.04
FV7_5_1P	200	-	425	74	0.50
FV6_2_1S	200	40	410	75	0.04
FV6_3_1P	200	-	428	75	0.50
FV6_8_1S	200	60	400	75	0.04
FV7_1_1P	200	-	469	74	0.50
FV8_1_1S	293	10	1700	81	0.04
FV8_2_1P	293	-	1772	81	0.20
FV7_3_1S	293	60	1700	74	0.06
FV7_4_1P	293	-	1740	74	0.20
FV7_1_3S	293	120	1500	74	0.07
FV7_2_1P	293	-	1741	74	0.40

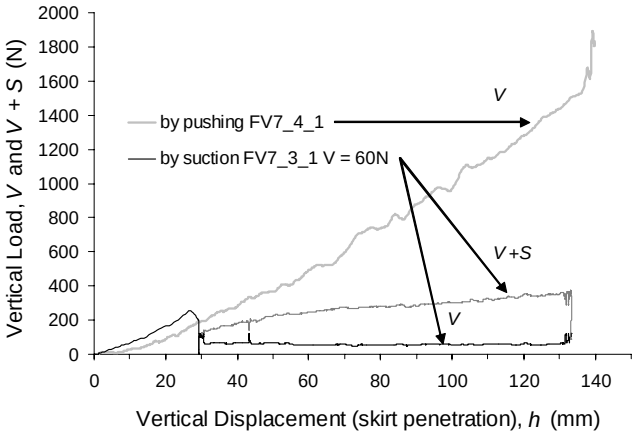

Figure 5: Comparison between pushed installation and suction installation for 293mm diameter caisson

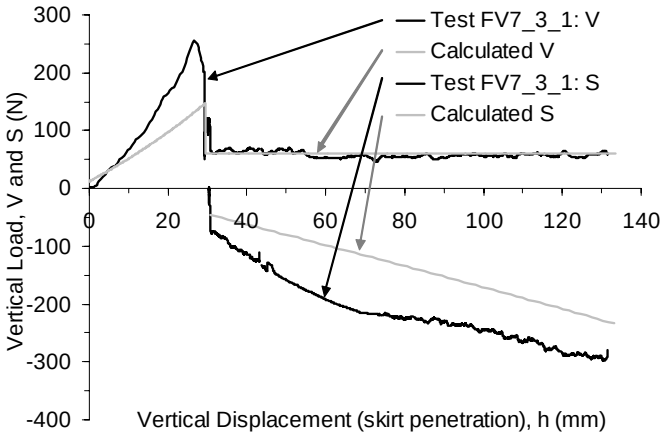

Figure 6: *V* and *S* comparison between experimental result and calculation for a suction installed test of the 293mm diameter caisson

Figure 5 shows the load penetration curves for a pushed test and a suction-installed test. In the latter the vertical load was kept constant at 60 N during the suction phase. For this test the curve labelled *V*+*S* shows the net vertical load due to applied load plus the pressure differential on the caisson lid. It is clear that there is a significant difference between this net vertical load and the vertical load for the caisson installed by pushing. The difference between these curves represents the beneficial effects of the hydraulic gradients set up within the soil due to the suction.

Figure 6 shows one of these tests compared to the theoretical predictions of Houlsby and Byrne (2005). In all of the experimental tests the suction was applied after approximately 30mm of penetration. The suction force shown in Figure 6 is slightly underestimated by the calculations.

5. MOMENT CAPACITY

Once the caissons were installed, moment capacity tests were carried out. These tests are similar to

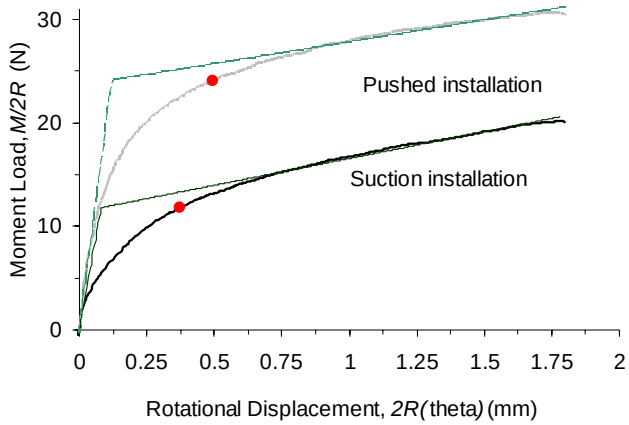

Figure 7: Moment capacity tests, load-rotation response showing yield points $(M/2R)_y$

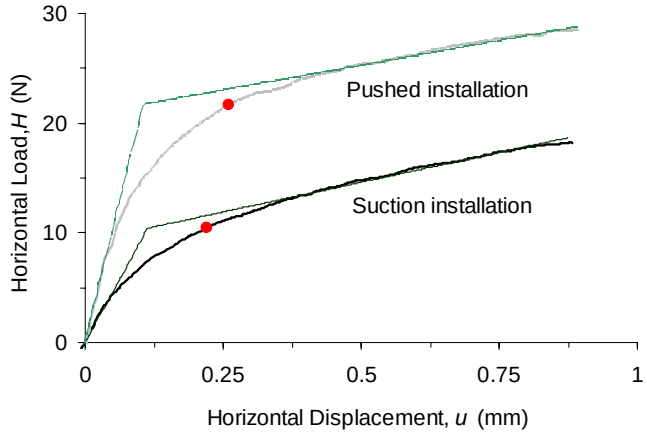

Figure 8: Two moment capacity tests, load-displacement response showing yield points H_y

those reported by Byrne *et al.* (2003), and consist of rotation and translation of the footing at a specified ratio of *M*/2*RH* under a constant vertical load. The tests were carried out slowly, so that the conditions were fully drained. They are thus relevant to only one of a series of possible conditions in the field, where, depending on caisson size, sand type and loading rate, conditions may vary from fully drained to almost undrained. Summary data for the moment tests are presented in Table 4, and further data about initial conditions can be found in Table 3 (installation method, V_o, initial R_d, *etc.*)

Figures 7 and 8 compare the moment and horizontal load capacities for different installation methods for the 200mm diameter caisson. It is clear from these figures that the installation method has a strong effect on the load-displacement behaviour. The load-displacement curves have been interpreted using the method described by Byrne *et al.* (2003), with fitting linear expressions to the elastic and plastic components of the curve. The intersection of the lines represents a yield point. These points are shown on the figure and given in Table 4 for all the tests.

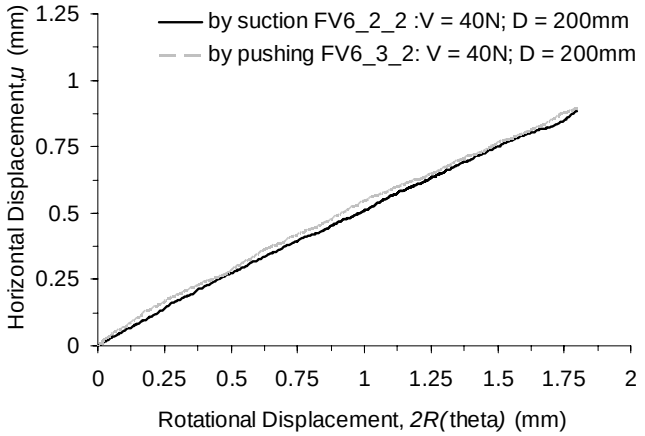

Figure 9: Plastic displacements increments during the tests: horizontal displacement with respect to rotational displacement

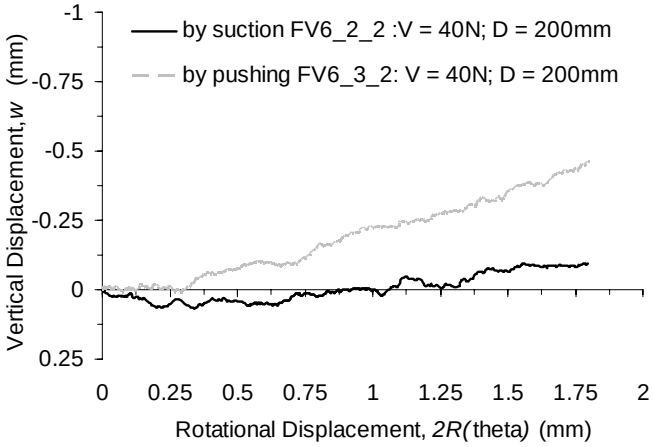

Figure 10: Plastic displacements increments during the tests: vertical displacement with respect to rotational displacement

The displacements paths from the tests are shown in Figures 9 and 10. In general the rotational displacement causes an initial elastic response that gradually changes to an almost perfectly plastic response, which can be fitted with a straight line.

The values of the slopes of these plastic displacement increments are presented in Table 4 as a ratio between horizontal and rotational displacement increments $\dot{u}/2R\dot{\theta}$ and between vertical and rotational displacement increments $\dot{w}/2R\dot{\theta}$.

Figure 10 illustrates the change of vertical displacement during the rotation of the caisson. The suction installed caisson experiences a lower magnitude of uplift compared with the caisson installed by pushing.

5.1 Yield Surface and velocity vectors

Using the yield points ($(M/2R)_y$, V) in Table 4, a plot of the yield surface for low vertical loads is illustrated in Figure 11. It is possible to fit through these data points a surface such as expressed by the formula:

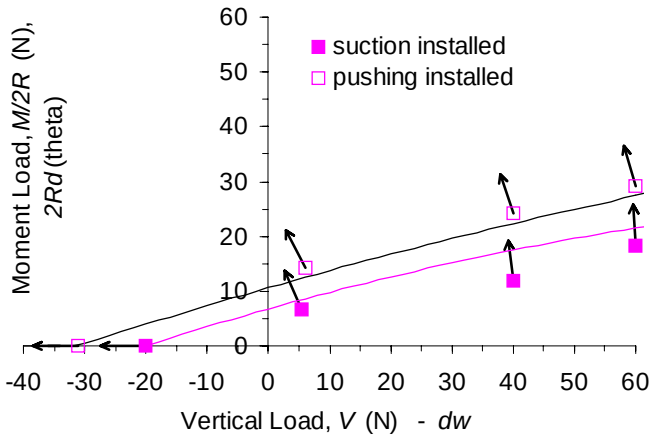

Figure 11: Pushing and suction installation calculations for a 200mm diameter caisson and V = 5N, 40N and 60N

$$y=\left(\frac{H}{h_oV_o}\right)^2+\left(\frac{M}{2Rm_oV_o}\right)^2-2a\left(\frac{H}{h_oV_o}\right)\left(\frac{M}{2Rm_oV_o}\right)- \left(\frac{\beta_{12}}{(t_o+1)^{(\beta_1+\beta_2)}}\right)^2\left(\frac{V}{V_o}+t_o\right)^{2\beta_1}\left(1-\frac{V}{V_o}\right)^{2\beta_2}=0 \quad (1)$$

in which $h_o, m_o, t_o, a, \beta_1$ and β_2 define the shape of the surface an $\beta_{12}=\frac{(\beta_1+\beta_2)^{\beta_1+\beta_2}}{(\beta_1)^{\beta_1}(\beta_2)^{\beta_2}}$.

Table 4: Moment capacity tests

Test	$\frac{M}{2RH}$	V N	$\left(\frac{M}{2R}\right)_y$ N	H_y N	$\frac{\dot{u}}{2R\dot{\theta}}$	$\frac{\dot{w}}{2R\dot{\theta}}$
FV6_5_2S	1.03	5.5	6.7	4.8	0.391	-0.397
FV7_5_2P	1.02	6	14.3	12.8	0.490	-0.445
FV6_2_2S	1.06	40	11.8	10.4	0.463	-0.122
FV6_3_2P	1.05	40	24.1	21.7	0.465	-0.284
FV6_8_2S	1.05	60	18.3	16.4	0.501	-0.051
FV7_1_2P	1.03	60	29.2	26.9	0.505	-0.253
FV8_1_2S	1.04	10	14.8	15.1	0.310	-0.409
FV8_2_2P	1.03	10	33.4	32.9	0.569	-0.551
FV7_3_2S	1.04	60	30.9	27.7	0.404	-0.299
FV7_4_2P	1.03	60	42.0	40.4	0.446	-0.483
FV7_1_4S	1.04	120	39.7	40.4	0.362	-0.125
FV7_2_2P	1.03	120	56.3	53.3	0.477	-0.289

The surface is fitted through the data points using parameter values given in Table 5. These values were found for a series of rotational tests performed with the same 293mm diameter caisson in dry sand. Also shown on Figure 11 are the directions of the displacement increment vectors.

The data for both footing diameters can be presented on the same figure by normalising with

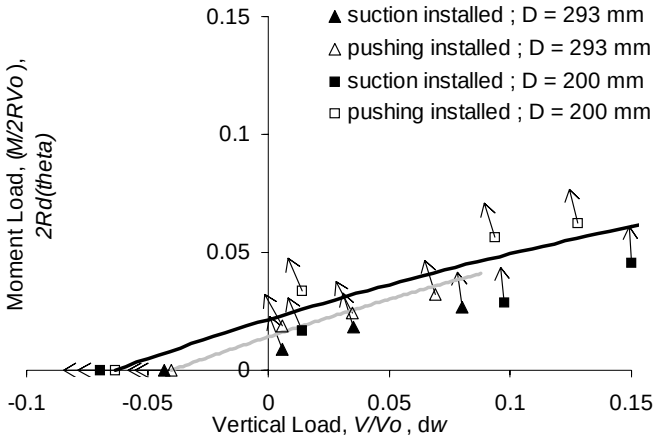

Figure 12: Summary of experimental yield points (normalized by V_o) and incremental plastic displacement vectors

respect to V_o, the maximum applied vertical load. These results are shown on Figure 12. Equation (1) has been included in this plot with a value of t_o = 0.064 for the smaller footing and 0.040 for the larger footing. It is necessary to use different values of t_o in this plot because the tensile capacity scales with $2RL^2$ whilst the V_o value scales principally with $2RtL$. Since the two footings have the same $L/2R$ value but different $t/2R$ values their tensile capacities differ on the normalised plot. However, the normalisation by V_o merges the two curves shown in Figure 11 for any one caisson, thus suction or pushing installation has only a minor effect on the normalised curve.

In more detail, however, the yield surfaces presented in Figure 12 serve as lower bounds for the moment capacity in the case of a caisson installed by pushing. On the other hand, it represents an upper bound for a suction installed caisson. The differences are thought to be due to disturbance in the installation process due to suction.

The incremental plastic displacement vectors were also compared. The vectors for suction installation tests have a smaller component in the *w*-direction compared with the vectors for pushed installation tests (see last column in Table 4 for values). Therefore, there was less uplift during the rotation of a caisson when a suction installation procedure was used.

Table 5: Yield surface parameters for $L/2R$ = 0.5

Eccentricity of yield surface, a	-0.75
Horizontal dimension of yield surface, h_o	0.337
Moment dimension of yield surface, m_o	0.122
Curvature factor at low V, β_1	0.99
Curvature factor at high V, β_2	0.99

6. CONCLUSIONS

A series of experiments comparing the moment response for suction installed caissons and those installed by pushing have been carried out. The main results are:

(a) The use of suction beneficially reduces the resistance to penetration of the caisson.

(b) The moment resistance of a suction caisson depends on the method of installation.

(c) The ratio of horizontal and rotational plastic displacement increments, $\dot{u}^p / 2R\dot{\theta}^p$, was independent of the installation method.

(d) Under rotations more vertical uplift was observed for the pushed installed caisson than the suction installed caisson although this was also dependent on the applied vertical load.

(e) The yield surface (equation (1)) was applied successfully to two different size suction caissons after normalisation by V_o, but requires differing values of t_o, to account for different ratios of *2R/t*.

REFERENCES

Bolton, M.D. (1986) The strength and dilancy of sands. *Géotechnique*, Vol 36, No. 1, pp65-78

Bye, A., Erbrich, C. T., Rognlien, B., and Tjelta, T. I. 1995. Geotechnical design of bucket foundations. *Offshore Technology Conference*, Houston, paper 7793

Byrne, B.W. 2000. Investigations of suction caissons in dense sand, DPhil thesis, University of Oxford

Byrne, B.W. and Houlsby, G.T. 2003. Foundation for offshore wind turbines, *Phil. Trans. of the Royal Society of London*, Series A 361, 2909-2300

Byrne, B.W., Houlsby, G.T., Martin, C.M. and Fish, P.M. 2002. Suction caisson foundations for offshore wind turbines. *Wind Engineering*, Vol. 26, No 3.

Byrne, B.W., Villalobos, F.A., Houlsby, G.T. and Martin, C.M. 2003. Laboratory Testing of Shallow Skirted Foundations in Sand, *Proc. Int. Conf. on Foundations*, Dundee, 2-5 September, Thomas Telford, 161-173.

Gottardi, G., Houlsby, G.T. and Butterfield, R. 1999. The Plastic Response of Circular Footings on Sand under General Planar Loading, *Géotechnique*, **49**, 4, pp 453-470.

Houlsby, G.T. and Cassidy, M.J. 2002. A plasticity model for the behaviour of footings on sand under combined loading, *Geotéchnique*, Vol. 52, No. 2, pp 117-129

Houlsby, G.T. and Byrne, B.W. 2005. Calculation procedures for installation of suction caissons in sand. *Proc ICE, Geotechnical Engineering*, in press

House, A.R. 2002. Suction Caisson Foundations for Bouyant Offshore Facilities, PhD thesis, the University of Western Australia

Kelly, R.B., Byrne, B.W., Houlsby, G.T. and Martin, C.M. 2004. Tensile loading of Model Caisson Foundations for Structures on Sand, *Proc. ISOPE. Conf.*, Toulon

Martin, C.M. 1994. Physical and Numerical Modelling of Offshore Foundations under Combined Loads, DPhil thesis, University of Oxford